05

Phase transitions in superconductors with current under non-uniform heat removal conditions

© V.A. Malginov,[1] L.S. Fleishman[2]

[1]Lebedev Physical Institute, Russian Academy of Sciences,
119991 Moscow, Russia
[2]Sergo Ordzhonikidze Russian State University for Geological Prospecting,
117997 Moscow, Russia
e-mail: malginovva@lebedev.ru

Received April 17, 2025
Revised June 3, 2025
Accepted June 3, 2025

A study was made of phase transitions to normal state in high-temperature superconducting wires with current due to gaseous nitrogen occurrence around some part of the wire. The simultaneous presence of liquid and gaseous refrigerant along the wire length means that heat removal non-uniformity from its surface takes place that results in normal zone formation in the wire with current in the site with reduced heat removal. As a result, a jump-like change in the current and voltage occurs that may be used for signal generation by a superconducting sensor in alarm level indicator and/or gaseous inclusion indicator in liquid nitrogen. The sensor's ability to work is based upon the wire normal state stability maintenance after its operation and upon the reliability of the transient signal registration from the low resistance normal region. These was realized by means of AC current measurements using a transformer-based power supply. The results obtained for the first time are presented of physical modelling of the transients in the superconducting sensors depending on a stabilizing layer presence in the wire, the current supply method (cooled/non-cooled leads), the wire structure (single/bifilar). The importance of the obtained results for applications is confirmed by the recommendations developed on their basis concerning the superconducting sensor application in the alarm indicators for the two types of nitrogen cryostats: bulk type (for winding refrigeration) or long type (cryostat shell for superconducting cable).

Keywords: high-temperature superconductor, phase transition, heat balance, normal zone, superconducting gaseous phase sensor.

DOI: 10.61011/TP.2025.11.62235.64-25

Introduction

A series of studies in the field of superconductivity applications is aimed at both reducing loss in electrical power devices [1,2] and ensuring the reliability and trouble-free operation of such devices [3]. To ensure normal operation, most superconductor devices intended for power supply require cooling preferably by a liquid cryogen due to heat release in AC mode. Moreover, liquid cryogen may help maintain stable overload condition [4,5] in superconducting wires carrying supercritical current in emergency operation mode. Special focus shall be made on superconducting current-limiting devices [6], whose performance is based on removal of heat release resulting from superconductor transition into a normal state, from „superconducting resistors" into a liquid cryogen [7]. It follows from the above that when a gas phase (gas bubbles, vapor locks) occur in a cryostat system for superconductor device treatment, the gas phase shall be promptly detected and a control alarm shall be sent to the control and automation system. This function may be fulfilled by gas phase sensors placed in a liquid-cooled cryostat. One of options for enabling an alarm in case of impermissible reduction of a cryogen level and/or formation of gas inclusions in a cryogen is based on a dramatic change of electrical properties of a superconductor during a phase transition from a superconducting state to a normal state (S-N transition). A physical mechanism initiating the S-N transition in a current carrying superconductor in this situation is nonuniform heat removal to the environment [8].

Cryostats for superconducting devices may be divided into two types depending on the intended use and design: bulk cryogenic vessels with a horizontal liquid level and long cryostats [9] (cryostatic shells in the terminology of [10]) for high-temperature superconductor (HTSC) cables similar to cryogenic piping where the whole volume is filled with a liquid cryogen. In the first case the required sensor will consist of an emergency level alarm, which is common for the whole vessel, and in the second case this will be an extended (distributed) sensor sensitive to local gas formation in some region over the cryostat length. Thus, there is a critical need for development and implementation of a gas phase alarm sensor concept for cryostat systems for superconducting devices.

It should be emphasized that requirements for a level alarm sensor differ fundamentally from those for cryogenic liquid level gauge sensors, which are widely used for cryogenic applications [10]. A level gauge sensor shall have a smooth uniform (preferably linear) dependence of the output signal on the cryogen level (a so-called voltage-level

characteristic). This is where the efforts of designers of various level gauges are fostered [11–27]. In contrast, a level alarm sensor shall have a stepped characteristic, i.e. generate an output jump when the cryogen level decreases below the allowable limit.

This study describes HTSC devices designed for power supply that are cooled by liquid nitrogen. HTSC materials are also appropriate as a sensitive element in this case. Operating principle of such HTSC gas phase sensor is based on the loss of thermal balance stability in a current-carrying superconducting wire followed by an abrupt transition to a normal state due to heat removal impairment when local gas medium appears in the vicinity of the wire [8]. Appearance of a normal zone in the HTSC wire followed by generation of an alarm/control signal serves as sensor „actuation". Real performance will be defined by actuation accuracy, reliability of electric alarm extraction from a steady-state signal, repeatability, unambiguous reference of sensor actuation to a particular liquid level regardless of power supply circuit parameters. Altogether, this constitutes transient characteristics of superconducting gas phase sensors, determination of which was the objective of this study. To meet this objective, experiments were conducted using superconducting sensor models furnished with transient process detection systems.

As described above, the operating principle of the sensors is common for various purposes, however, particular conditions of use in bulk and long nitrogen cryostats have a number of fundamental differences. Therefore, further description contains sections addressing each of the potential sensor applications, i.e. either as a liquid nitrogen level alarm in a cryogenic vessel or as a gas phase sensor in a long nitrogen cryostat. Introduction to each of these sections describes the current state of art in this field of research and defines the problems to be solved.

Electrical measurements of transient processes in various sensor versions used a common technique, which is described below.

1. Normal zone formation conditions and method for investigating phase transitions in current-carrying HTSC wires

For transition of type-II superconductor from a superconducting (S) state to a normal (N) state, it is necessary that either its temperature exceed the critical value or a magnetic field exceed the upper critical field value (which is extremely difficult to achieve because it is great in magnitude). Transport current may also initiate the S-N transition, however, it is done indirectly: when the critical current is exceeded, dissipative resistive state occurs and may cause superconductor heating above the critical temperature [28]. Since HTSC wires with various layouts have the best prospects of superconductivity applications in electrical engineering, it is HTSC wires that will be discussed below, and the term „superconductor" will be often used for brevity (and to avoid repetition). Propagation of a transient process initiated by the transport current in a superconductor is defined by the presence/absence and thickness of a stabilizing layer/matrix with high conductivity [29]. When there is no stabilization, the S-N transition takes place with slightly exceeded critical current. When there is a stabilizing layer with a sufficient thickness in a current range (from the critical current to thermal breakdown current), a so-called stable overload condition [4,5] of a superconductor occurs in the resistive state below the critical temperature.

In practice, superconducting sensors/level alarms use the first (heating) and/or the last (transport current) from the three above-mentioned S-N transition methods. In the first case, the superconductor is furnished with an electric heater, power of which shall be selected in such a way that the S-N transition is provided only in the superconductor portion surrounded with gas [11,12,18]. For a distributed gas phase sensor, such heating method is unacceptable, because when the cryostat/HTSC sensor length and, consequently, the heater length is equal to several hundreds of meters, thermal load on the cryogenic system will increase considerably. Another method (i.e. through the transport current) works due to the local heating capability of the superconductor in a reduced heat removal region. Moreover, the remaining HTSC wire length is in the superconducting state without inducing the above-mentioned heat load.

In case of similar heat removal conditions throughout the superconductor surface, localization of normal phase nucleation in the wire when the critical current is exceeded is defined by a „weak spot" (i.e. a region with reduced superconductor parameters). In contrast, when there is nonuniform heat removal, for example, due to nitrogen vapor near the superconductor, bonding pads with current leads, etc., a region with reduced heat removal and/or increased temperature, where the normal phase is generated, is a „weak spot". If the nucleation of this phase is detected, then a signal of gas medium formation in a liquid cryogen may be generated, and this is exactly required from the gas phase sensor. If, after normal phase nucleation, causes/conditions for normal phase existence/proliferation/propagation remain effective, then a (stationary or propagating) normal phase is formed in the superconductor [28,30]. Transport current flow over the normal zone may cause overheating and irreversible superconductor degradation. To avoid this, the current shall be reduced considerably and rapidly enough.

Thus, to investigate the phase transition in the current-carrying HTSC wire (from the standpoint of future utilization in superconducting sensors), the problem of prompt detection of the normal zone occurrence and the problem of rapid current reduction in the wire shall be solved. Both problems are nontrivial, i.e. the superconductor, including the normal zone, has a quite low resistance during DC measurements due to the presence of a conducting substrate/matrix/stabilizer and/or to a small size of the

normal zone. Therefore, being a load for DC power supply, the superconductor cannot affect the DC magnitude in the circuit during a local transition to the normal state. Nevertheless, self-induced power supply current reduction may be achieved at a particular moment, if an AC measuring circuit is used, as was the case in this study.

The key factor for achievement of the result — current drop during the phase transition in the superconductor — is utilization of a transformer power supply circuit: the HTSC wire is connected directly to low voltage (LV) winding outputs of a stepdown transformer (ST). When such connection is used, impedance of the HTSC wire segment in the superconducting state (inductive reactance) is inherently lower than the secondary winding impedance of ST, whose operation in this case is known as a transformer short-circuit condition [31], and the whole power supply circuit is used as a controlled current source (current stabilization mode). Current may be controlled by varying the ST input voltage in the high voltage (HV) winding. If a phase transition takes place and the normal zone is formed in the HTSC wire, then, with the ST design parameters being chosen properly, active resistance of the wire after the S-N transition will considerably exceed the transformer source impedance, so it becomes a controlled voltage source (voltage stabilization mode). Owing this, the HTSC wire power supply current is significantly reduced due to the increased resistance, thus preventing from wire overheating and failure and simultaneously allowing the phase transition event to be detected. Voltage in the wire naturally increases, but the voltage limit is controlled through the ST input voltage control. An allowable HV/LV range, where superconductor degradation/failure doesn't take place, may be defined by way of experiment. It is this method for investigating phase transitions that has been used in this study, and findings are described in detail below.

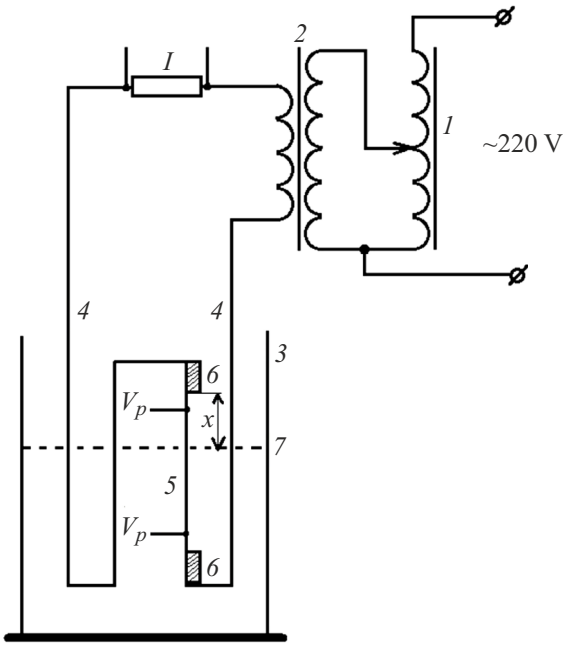

Figure 1. Measuring circuit: *1* — autotransformer, *2* — stepdown transformer, *3* — nitrogen cryostat, *4* — current leads (liquid nitrogen cooling option for the top current lead is shown), *5* — HTSC wire sample, *6* — contact clamps, *7* — liquid nitrogen level. I — circuit current, V_p — potential probes.

Measuring circuit for short vertical HTSC wire samples is shown in Figure 1. Such system is used for physical simulation of the liquid nitrogen level alarm HTSC sensor in a bulk cryostat. Simulation of the HTSC sensor in an long cryostat used a horizontal superconductor configuration [32]. Experimental cryostat ensures visual monitoring and detection of the liquid nitrogen level and position relative to the top end of the sample using the external scale. As the liquid nitrogen level decreases, the upper point of the sample was the first to enter the gas phase, after which the „exposed" (i.e. not immersed in the liquid) length x gradually increased. Measurements were made at commercial frequency alternating current (50 Hz). Second-generation HTSC wire (2G HTSC [33]) samples: length $L \approx 71 \cdot 10^{-3}$ m, width $b = 12 \cdot 10^{-3}$ m, Hastelloy substrate thickness $a_{Ha} = 60 \cdot 10^{-6}$ m, critical current $I_c(77\,\mathrm{K}) = 375 - 385$ A), were made of SuperOx 2G HTSC multilayer tape conductor [34]. Potential probes were soldered to the samples in a length of $61 \cdot 10^{-3}$ m and at distance of $5 \cdot 10^{-3}$ m from the sample ends. I — is the signal from the shunt resistor proportional to the current, V_L — is the voltage signal from the whole sample, V_p — is the signal from potential probes.

2. Characteristic of HTSC wire modes depending on the current load and heat removal behavior

When the transport current is introduced into the HTSC wire, electrical and thermal states of the superconductor change and each of them characterizes a certain current-carrying wire mode. Feasibility of a particular mode is defined by the wire layout and heat removal conditions. Full mode change sequence may be observed more vividly through volt-ampere characteristic (VAC) measurement. During AC measurements, VAC are determined by signal amplitude values (amplitude VACs). For a non-linear conductor, which is the superconductor, current and voltage signals in some modes are non-sinusoidal, and maximum currents throughout each period are used for plotting amplitude VACs. A VAC thus plotted enables some superconductor properties to be identified: impedance in a linear segment, critical current, thermal breakdown current.

Measurement technique used in this study included detection of instantaneous electrical signals with a time resolution of 0.5 ms. Thus, besides VAC construction, one of three possible modes of the superconductor could be identified (Figure 2).

First, this is a stable superconducting mode where the superconductor state remains unchanged over time, and electrical signals have a steady-state value regardless of

the heat removal behavior. Initial linear segments of VAC correspond to this mode where the impedance is inductive reactance and AC heat release in the superconducting state is negligible [35]. Critical current of the HTSC wire may be determined by VAC deviation from the linear extrapolation of this segment (shown in Figure 2).

Second, this is an overloaded mode in the range from the critical current to thermal breakdown current where this range may have a considerable length if the wire is stabilized and fully immersed in liquid nitrogen. Such situation was studied in detail in [5], and is shown in Figure 2 as curve *1* where the overloaded mode corresponds to a non-linear portion of VAC. Thermal breakdown current for this VAC is 600 A, therefore (due to the need for choosing scales/limits on axes for curves *2* and *3*) the thermal breakdown point is not shown on curve *1*. The AC overloaded mode was theoretically studied in [4] where it was shown that such mode in HTSC wires may be stable and transition to this mode may be free from transit-time effects (i.e. synchronous with current rise). In [4], a mathematical model of the overloaded mode with a single heat removal mechanism was developed. However, the mechanism of heat removal from the superconductor surface to liquid nitrogen changes from convection [36] to nucleate boiling [37] as heat releases increase, and the change of this mechanism takes a particular time necessary for nucleate boiling activation [38]. Therefore, in some current range, an overloaded mode instability may be observed and is displayed in irregular current and voltage signals and in an irregular region occurring on VAC [39]. There is such region on curve *1* Figure 2. The described instability is damped, and the heat removal mechanism variation process is ended by a change to the steady state [29].

Third, it is a transient mode after passing the thermal breakdown point where the wire is in heat disbalance state. In this mode, S-N transition takes place both when the HTSC wire is fully immersed in liquid nitrogen (not shown on curve *1* due to the chosen limited range of axes in Figure 2) and when there is an „exposed" wire segment (curves *2* and *3*). In the transient mode, signal amplitudes vary between periods. Corresponding points on VAC represent a sequence of amplitudes in each period with current drop and voltage growth during the transient process, whilst the transition branch of VAC is non-stationary and has a negative slope (curves *2* and *3*).

Transient process outcome depends both on the measurement method and heat removal conditions. In the measurement technique where the input voltage of the superconductor energizing circuit is gradually increased, VAC slope increases and the transient process is not stopped (curve*2*), which finally, if the driving voltage rise is not stopped, leads to irreversible superconductor degradation due to thermal damage of its local „hot zone". When the power supply system is allowed to change to another state spontaneously after thermal breakdown (with fixed ST input voltage and sample resistance rise, due to which the power

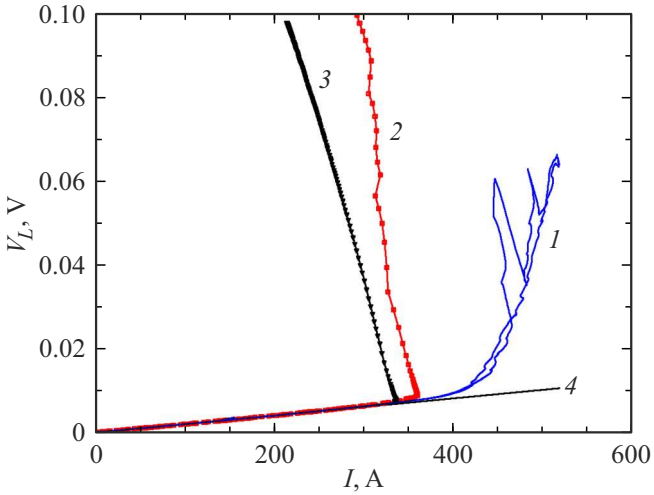

Figure 2. Amplitude VAC of the stabilized HTSC wire sample: *1* — the sample is fully immersed in liquid nitrogen, *2* — exposed length $x = 33$ mm, controlled power supply voltage mode, *3* — exposed length $x = 22.5$ mm, fixed power supply voltage mode, *4* — linear extrapolation of the superconducting VAC segment.

supply (Figure *1*) changes from the current stabilization to voltage stabilization mode), then (with particular limitations of the initial exposed wire length x) the S-N transition ends with a new stable mode with reduced current and increased voltage on the superconducting wire, a part of which is in the normal state. The upper point on the „inverse" branch (i.e. a transient negative slope branch) on curve *3* corresponds to this stable state on VAC. By measuring VACs similar to that shown on curve *3*, conditions, in which the S-N transition will be reversible, may be identified to reproduce these conditions in future for investigating physical models of HTSC sensors. In one of them, the sensor shall respond to a particular position of the gas-liquid interface of nitrogen in the vertical bulk cryostat, in the other, the sensor shall respond to occurrence of such interface in a random area of the horizontal long cryostat.

3. Transient processes and heating during phase transitions in vertical current-carrying HTSC wires intersecting the liquid nitrogen surface

3.1. State of the art and research problem statement

In [8], the authors proposed an operating principle of a superconducting alarm level detector for liquid nitrogen and demonstrated its performance using a physical model. In contrast to electrical level sensors (including a superconductor sensor) having a smooth voltage-level characteristic, the alarm sensor gives abrupt voltage variation as the level decreases below the permissible limit. However, the superconducting and normal states of the sensor (before

and after actuation) shall have sufficient stability to avoid false actuations and/or resetting.

With the pre-defined initial current, the alarm sensor is actuated (i.e. changes to the normal state) with a particular length of the external HTSC wire segment (above the nitrogen level and exposed to nitrogen vapor). For details of the transient process, see [8]. It is also shown there that repeatability is acceptable for the HTSC transformer winding cryostat systems. In [8], measurements were conducted in boiling liquid nitrogen at atmospheric pressure and, consequently, at a fixed cryogenic liquid temperature. Cryogenic treatment in boiling nitrogen is used in such types of HTSC electric devices where the presence of vapor above the liquid doesn't deteriorate their performance, for example, for cryogenic treatment of HTSC windings of a transformer [40] or current limiter [6].

The external length during actuation is defined by both sensor design and heat removal conditions. In [8], conditions for maximum stabilization of superconducting state during nitrogen level reduction were created: presence of Cu-stabilizing layers in the HTSC wire and liquid nitrogen cooling of the top and bottom current leads (by passing a portion of the top current lead through a nitrogen bath below the HTSC component). Longitudinal thermal conductivity [41] provided superconducting state stability in a particular external length range and ability to change this length as the initial current varies.

To find the best sensor actuation version during reduction of liquid nitrogen level, this study investigated the transient process and evaluated the maximum heating level during phase transition in a vertical stabilized/non-stabilized second-generation (2G) HTSC wire with two current lead methods, i.e. with top current lead with (Figure 1)/without liquid nitrogen cooling.

3.2. Measurement results and discussion

Measurements used a technique described in Section 1 with four possible stabilizing layer options in the HTSC wire and current lead methods as shown in Table 1.

Figure 3 shows how voltage (Figure 3, *a*) and current (Figure 3, *b*) amplitudes vary as the liquid nitrogen level decreases in each of the options. Curves *1* correspond to „actuation" of the stabilized HTSC wire with cooled current leads, which was addressed in [8]. Curves *2* for an option without the top current lead passing through the nitrogen bath demonstrate a qualitative difference from option 1, i.e.

Table 1. Measurement options for the vertical HTSC wire

Option No.	1	2	3	4
Two-layer Cu-stabilizer $2 \times 20\,\mu$m in the HTSC wire	+	+	−	−
liquid nitrogen cooling of the top current lead	+	−	+	−

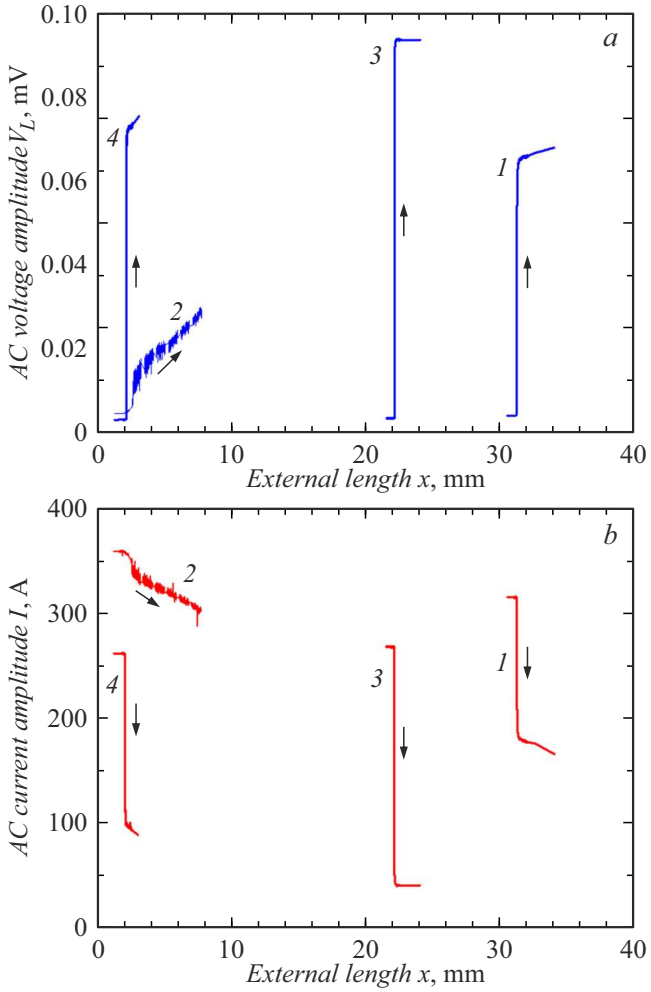

Figure 3. Dependences of the voltage and current amplitudes on the external („exposed") wire length x as the liquid nitrogen level decreases; *a* — voltage of the total wire length V_L, *b* — current I. *1–4* — measurement options.

changes in current and voltage amplitudes start almost immediately after „exposure" of the HTSC wire. The changes occur gradually without a clearly pronounced „actuation" and are followed by irregular fluctuations resulting from instable change of the non-superconducting wire portion boundary due to vigorous nitrogen boiling. Amplitude if these irregularities decreases as the „exposed" length increases due to reduction of the relative proportion of the near-surface resistance. Curves *3* and *4* are qualitatively similar to curves *1* with stepped voltage-level characteristic.

Since the exposed wire temperature gradually increases as the nitrogen level decreases (x increases), actuation is induced by transition of this segment in nitrogen vapor from the superconducting to normal state when the critical temperature is reached exactly in this section (such transition may be called a „thermal" transition in contrast to a resistive one, i.e. induced by exceeding the critical current). Amplitude VAC of the wire fully immersed in liquid (curve *1*) in Figure 2 demonstrates a resistive

transition, and VAC of wires with an exposed segment (curves *2* and *3*) demonstrate a thermal transition. During thermal transition, current range with resistive state is very small, and for options 1, 3, 4 of wire layouts/current lead connections (Table 1), voltage and current surges occur as x is varied, which is typical of transition to the normal state (Figure 3, curves *1*, *3*, *4*). Since the initial inductive voltage is max. 10 mV (with inductive reactance in the length of $61 \cdot 10^{-3}$ m is 12.2 $\mu\Omega$, and the inductive reactance per unit length is at 200 $\mu\Omega$/m), voltage surges are much higher than the inductive voltage level and are resistive. As for the transition in option 2, it starts when the wire top is exposed, but cannot take place immediately because top heating due to uncooled current lead competes with bottom cooling through the liquid-immersed Cu stabilizer. Therefore the transient process is delayed and curve *2* in Figure 3 serves as an example of a version that cannot be used in the liquid nitrogen level alarm sensor. However, for the non-stabilized wire (option 4) that has high resistance of non-superconducting layers, transition of even several millimeters of wire, when the bottom end of the current lead is exposed, induces a voltage/current surge sufficient to act as a sensor actuation signal (curve *4*).

To determine failure protection of HTSC sensors, estimate the temperatures that can be reached during actuation. HTSC tape heating after S-N transition may be estimated by comparing experimental resistances and dependence on temperature for individual tape wire components as specified in handbooks. Reference measurement of resistance was conducted at 20 °C. It was established that the effective thickness of Cu/Ag stabilizer $2a_{\mathrm{Cu}}$ in the stabilized tape was $44.5 \cdot 10^{-6}$ m, protective Ag layer thickness in the non-stabilized tape was $2a_{\mathrm{Ag}} = 4.5 \cdot 10^{-6}$ m. Hastelloy substrate layer measurements have shown that Hastelloy resistivity was $\rho_{Ha} = 101 \cdot 10^{-8}\ \Omega\cdot$m and virtually independent of temperature.

Since the stabilizer layer and substrate layer are connected in parallel, after transition to the normal state in the approximation of heating to the maximum temperature T_m over the length of a segment with the normal zone length L_N, a definite correlation may be determined between the stabilizer resistivity $\rho(T_m)$ and impedance Z (that may be set equal to the active resistance for semiquantitative estimation) after the S-N transition:

$$\rho(T_m) = \frac{\rho_{Ha} 2aZ}{\rho_{Ha} L_N / b - a_{Ha} Z}, \qquad (1)$$

where $b = 12 \cdot 10^{-3}$ m is the tape width, $a_{Ha} = 60 \cdot 10^{-6}$ m is the substrate thickness, $2a$ is the protective layer and stabilizer thickness (or only protective Ag layer thickness in non-stabilized tapes). Resistivity (in $10^{-8}\ \Omega\cdot$m) of the Cu/Ag stabilizer of stabilized HTSC tapes has the following reference temperature dependence [42] ($T_0 = 77$ K) experimentally clarified for HTSC tapes [43]:

$$\rho_{\mathrm{Cu}}(T_m) = 0.22 + 0.0072(T_m - T_0). \qquad (2)$$

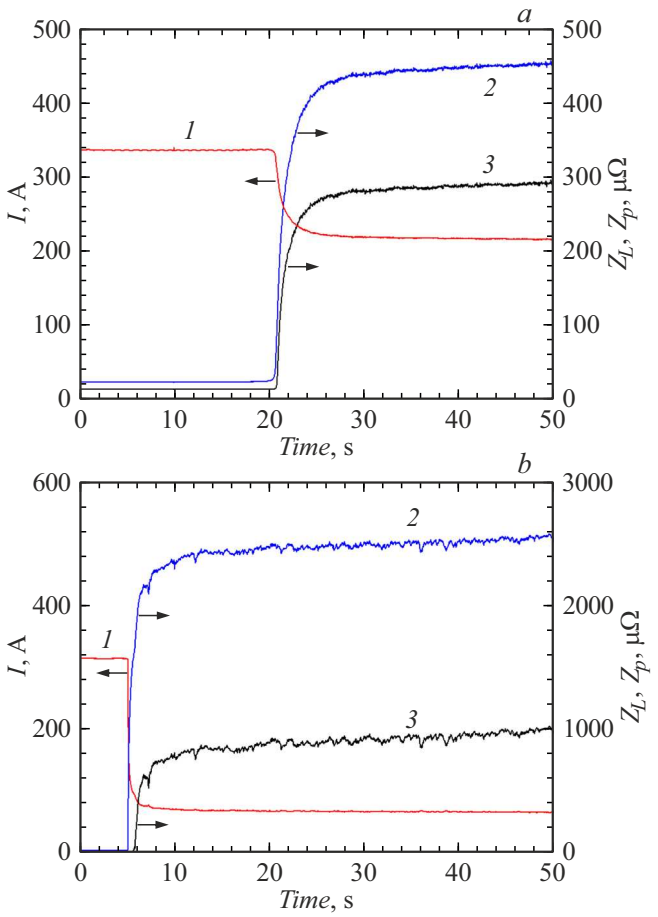

Figure 4. Time dependences of current and resistances of different HTSC wire sample segments during the S-N transition induced by liquid nitrogen level reduction: *1* — current amplitude, *2* — resistance of the whole sample Z_L, *3* — resistance of the sample interior Z_p; *a* — the sample with the Cu stabilizer, *b* — the sample without stabilizer.

A similar expression for resistivity of the protective Ag layer of non-stabilized HTSC tapes is written as:

$$\rho_{\mathrm{Ag}}(T_m) = 0.29 + 0.0061(T_m - T_0). \qquad (3)$$

Temporal behavior of Z after actuation for different types of tapes is shown in Figure 4. Curve *2* is the full sample length resistance Z_L, curve *3* is the resistance between potential contacts Z_p in the length $L_p = 61 \cdot 10^{-3}$ m, vertical difference between curves *2* and *3* shows resistance of segment $L_{up} = 5 \cdot 10^{-3}$ m located near the top sample end. It follows from the figure that the normal zone rapidly fully fills the exposed segment L_{up}, and its resistance (vertical difference between curves *2* and *3*) is almost stabilized after 5–10 s (meaning that a steady-state temperature is reached in this segment). Sample impedance continues growing synchronously with nitrogen level reduction and wire „exposure“ at a rate of 1 mm/s. Thus, the normal zone size during phase transition is limited by the exposed wire segment with low heat removal to the surrounding nitrogen vapor. At the same time, the normal zone doesn't

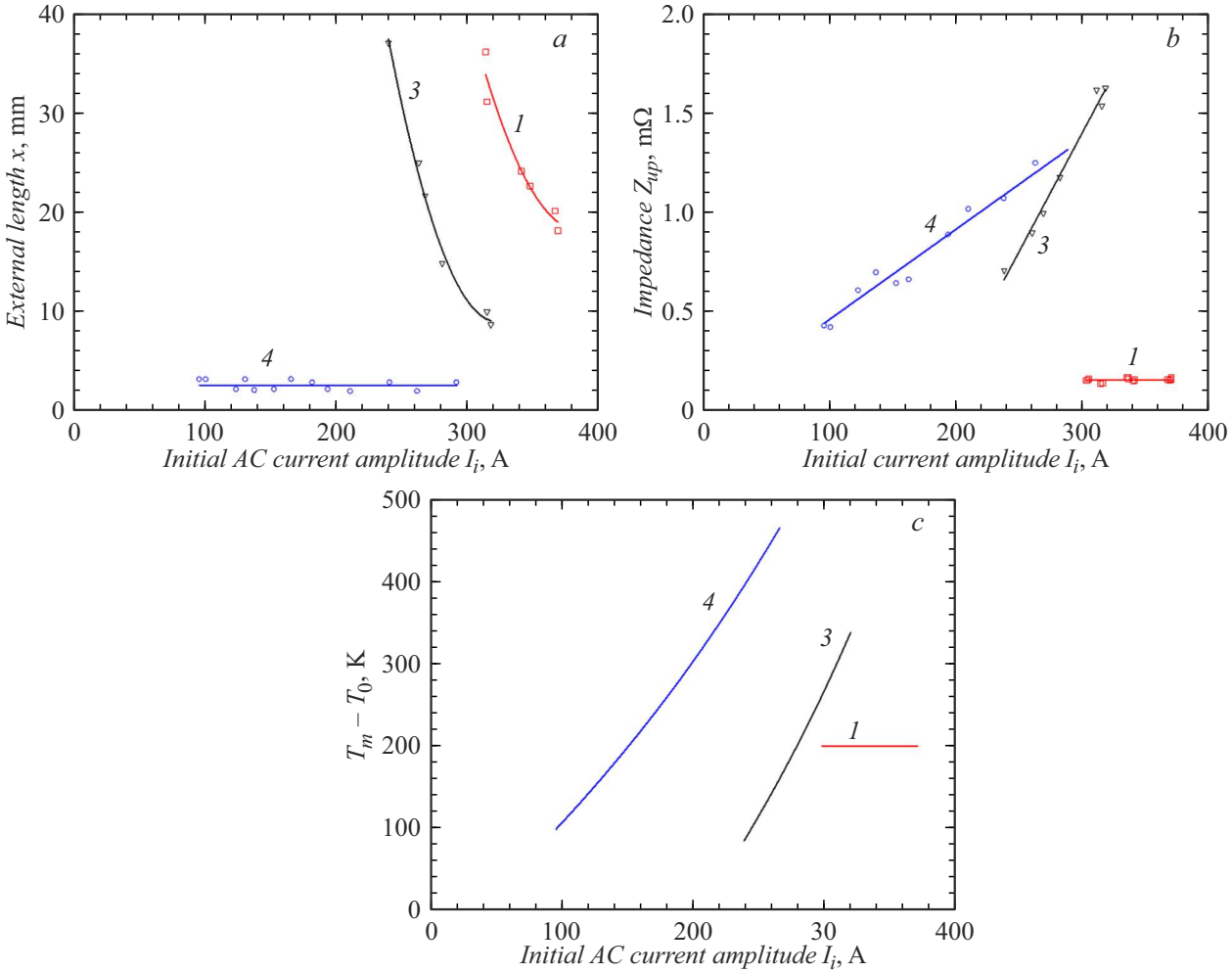

Figure 5. Dependence of parameters during actuation on the initial current amplitude I_i; *a* — external length x; *b* — wire segment resistance Z_{up}; *c* — sample overheating after actuation. *1*, *3*, *4* — measurement options.

get into the segment wetted with liquid nitrogen due to the current drop and high heat removal from the surface. Since transitions start at the top sample end and it has been clearly established that the small segment L_{up} is fully filled with the normal zone, the mean temperature in this segment is close to maximum overheating and may be most reliably described by expressions (1)–(3). It also follows from Figure 4, *b* that contribution of the normal resistance in the segment L_{up} for the non-stabilized tape is much higher than for the stabilized tape. Consequently, near the maximum heating level, temperature gradient along the wire will be higher for the non-stabilized tape.

Substituting the numerical values of $2a$, b, $L_{up} = 5 \cdot 10^{-3}$ m and $\rho(T_m)$ from (2) and (3) into (1) in the approximation of uniform tape heating in this segment up to T_m, we get empirical dependences of HTSC tape overheating temperature with respect to liquid nitrogen temperature T_0 on Z_{up} (in Ω) in the segment L_{up}.

For the stabilized tape:

$$T_m - T_0 = 139(74.3Z_{up}/(0.00696 - Z_{up}) - 0.22), \quad (4)$$

for samples without Cu stabilizer

$$T_m - T_0 = 164(7.62Z_{up}/(0.00696 - Z_{up}) - 0.29). \quad (5)$$

For the current lead from top without liquid nitrogen cooling (option 4, Table 1), actuation takes place at any current near the bottom end of copper bus of this current lead (Figure 3, Figure 5, *a*), and there is no reliable information about the normal zone size in the steady state after actuation, therefore, it is suggested in this case that after actuation the normal zone occupies the exposed segment, which will be 3 mm long during the period when the temperature reaches the steady-state value and at a nitrogen level reduction rate of 1 mm/s. In such approximation, the quantitative estimation of overheating will be as follows.

For samples without Cu stabilizer, $L_{up} = 3 \cdot 10^{-3}$ m

$$T_m - T_0 = 164(7.62Z_{up}/(0.00417 - Z_{up}) - 0.29). \quad (6)$$

Operating current is one of the main parameters defining the operating mode when using superconducting devices. Dependences of actuation and transition characteristics on

the initial current amplitude I_i in our case are shown in Figure 5. Measurements of transition curves similar to those shown in Figure 3 are used to plot the dependences of the external length x during actuation on the initial current amplitude I_i for options 1, 3 and 4 (Figure 5, *a*). It follows from this figure that easily explainable and qualitatively similar dependences with decreasing actuation length as the initial current increases are obtained for options 1 and 3. However, the external length where the heat balance may be maintained at the defined current until the loss of superconductivity is smaller for option 3 than for option 1, and is smaller by an order of magnitude for option 4 and is almost independent of the initial current level. In this case the averaged x is 2.43 mm, and the normal zone size during transition is at $3 \cdot 10^{-3}$ m. Options 1 and 3 are characterized by the existence of a stable superconducting state in some „exposed" wire length range, this state ends with a so-called thermal breakdown, after which the temperature increases above the critical superconductor temperature. Such actuation mechanism (that is referred above to as the„thermal" mechanism) is also typical of options 2 and 4 where the top wire end temperature rapidly approaches its critical value when the bottom current lead edge is slightly exposed. Difference in x for different current lead connection options indicates different sources of sample temperature formation before actuation. In options 1 and 3, the exposed sample length acquires the temperature of the surrounding nitrogen gas. And in options 2 and 4, the top sample end temperature is formed by the heat flux from the current lead located in more heated nitrogen vapor. Figure 5, *b* shows the dependence of Z_{up} on I_i in the segment with $L_{up} = 5 \cdot 10^{-3}$ m with maximum heating near the top sample end for different measurement options. Using these resistances and equations (4)–(6), maximum heating was estimated in the steady state depending on the initial current amplitude. These dependences are shown in Figure 5, *c*.

3.3. Conclusions

The chosen sample power supply method that provides current reduction in the wire in transition to the normal state and the obtained data (Figure 3 and 5, *a*) suggest that various options (Table 1) may be used for the development of vertical gas phase sensors. First, liquid nitrogen cooling of both current leads defines the dependence of the „exposed" segment temperature on the surrounding vapor temperature and provides the superconducting state stability of the HTSC wire in an external length range whether or not there are Cu-stabilizing layers (versions 1 and 3). Option 1 is more suitable for short sensors (implementation conditions are described in [8]) — sufficient signal for actuation (Figure 3) and overheating protection (overheating is at 200 K (Figure 5, *c*)). Option 3 is more suitable for distributed sensors (implementation conditions are described in [32]) because it can produce a large amplitude signal (Figure 3), which is more easily extracted against the background of signals of different origin, which are independent of the S-N transition, from extended segments. Second, superconductivity stabilization is impossible in the exposed wire segment if cooling of only bottom wire is provided. In this case, for the sample with Cu stabilizer (option 2), occurrence of the normal zone in a small segment doesn't provide sensor actuation, resistance grows gradually as the nitrogen level decreases and resistive segment length increases. For the sample without Cu stabilizer (option 4), transition into the normal state is defined by heat input from the current lead, weakly depends on the initial current level and occurs „thermally" as soon as liquid nitrogen get down below the current lead end. This leads to transition of the small superconductor end and alarm actuation at the same nitrogen level with different initial currents. Such type of actuation offers the opportunity to use this option for vertical cryostats with cryogen temperatures and pressures varying during operation (i.e. containing so-called „underheated" liquid nitrogen without boiling due to excess pressure [1]). This option entails a risk of thermal damage of the wire if the initial current is in the upper half of the current range (Figure 5, *c*, curve *4*). Thermal load on the sensor wire may be reduced with preservation of alarm functionality by using the operating current below 200 A.

4. Transient processes and lateral heat transfer in current-carrying bifilar HTSC wires in liquid nitrogen containing gas inclusions

4.1. State of the art and research problem statement

Long cryostats for HTSC cables are fully filled with liquid nitrogen in the standard mode. If a local gas inclusion occurs in the cryostat for any reason, this may induce an abnormal/emergency mode due to disturbance of the cable temperature conditions resulting from heat removal deterioration. To ensure prompt response to gas inclusions (bubbles, vapor locks [44]) occurring in the cryostat, a gas phase alarm sensor shall be created for the long cryostat configuration. To date, distributed fiber-optic temperature sensor solutions having high temperature sensitivity and good local resolution have good prospects of application [45–47]. However, such sensors cannot function as gas phase alarm sensors due to their principle of operation. First, even when all calibration problems [45,46] are solved, temperature variation detection capability doesn't necessarily implies gas inclusion detection: cryogen for vapor inclusion prevention in the cable path is used in the above-mentioned „underheated" liquid nitrogen mode [1], therefore, it may have a varying temperature (below the saturation temperature) depending on the electrical load on the cable. Second, nitrogen vapor temperature difference inside the local gas phase from the liquid temperature is negligible. Consequently, a considerable difference in the properties of liquid and gas phases shall be used in

the sensor's operating principle. This is the capability to remove heat from the heat-releasing object surface. This difference means that heat removal is nonuniform for the extended sensor in the cable cryostat, and the best sensor performance will be achieved when heat release takes place exactly in the sensor segment that is surrounded by the gas phase. Operating principle of a sensor using a current-carrying HTSC wire where this condition is met was proposed in [32], where experiments on a physical model with a limited sensor length (about 1 m), which confirm the sensor functionality, are described.

This study continues study [32], i.e. is focused on a set of problems to be solved for justification of the HTSC sensor scalability to the long cable cryostat length (several hundreds of meters [1]). First, due to the need for AC measurements (Section 1), the inductive reactance (that is not changed in the S-N transition) of the sensor shall be minimized through using a bifilar wire. Second, electrical insulation between the bifilar wires shall be made in such a way that the induced delay in the alignment of high temperature (that occurs during phase transition) between wires in transverse direction is as low as possible. Third, it is necessary to provide mechanical stabilization of the bifilar wire, which is complicated by the interaction between parallel currents, in particular, when there are high magnetic field gradients near the edges of 2G HTSC tape wires [48]. Solution of the above-mentioned problems is the objective of this study.

4.2. Measurement results and discussion

Data obtained for the repeatable phase transitions in vertical HTSC wires in gas medium give grounds for using these materials in distributed horizontal gas phase sensors. One of the problems in the achievement of the necessary sensitivity of such equipment is the presence of signals, which are independent on the S-N transition (in particular, inductive voltage in the direct wire) and grow as the sensor length increases (effective signal in this case depends on the volume of HTSC materials in gas medium and doesn't depend on the total sensor length). Bifilar connection of wires with opposite currents is used to neutralize this voltage component.

For preliminary performance test of the bifilar wire, two non-stabilized tapes in the length of 100 mm were placed in our case horizontally with the HTSC layers facing each other. A 0.1 mm wire mesh insulation was placed between the tapes [49]. After the bifilar segment, the HTSC tapes proceeded to current leads. Vertical distance between these wires was 10–20 mm, and the total HTSC wire length between the bifilar segment and current leads was 200 mm. A signal (with the amplitude V_{bif}) was detected from the bifilar segment. A total voltage (with the amplitude V_{tot}) from the bifilar segment and wires leading to it was detected on the wire ends. The first experiments have shown that, when current is supplied to the sample, the top and bottom bifilar tapes are shifted relative to each other. To reduce this effect and fix the tape positions, the tapes were further clamped between horizontal adhesive tapes. Amplitude VAC for the prepared sample is shown in Figure 6. The left-hand V_{tot} axis and curve *1* show the total signal behavior. The right-hand V_{bif} axis and curve *2* show the voltage amplitudes on the bifilar segment. Curves *3*, *4* are the extrapolation of initial segments of experimental curves by a linear function and show the inductive signal level.

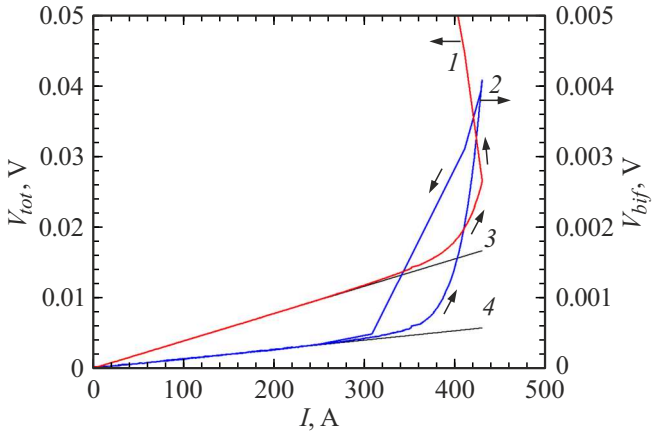

Figure 6. Amplitude VAC of the sample with a bifilar segment in liquid nitrogen: *1* — total signal, *2* — signal from the bifilar segment, *3* — $V_{tot} = 38.7 \cdot 10^{-6} I$, *4* — $V_{bif} = 1.33 \cdot 10^{-6} I$.

Comparing the VAC behavior of a single tape (Figure 2, curve *1*) and the bifilar sample (Figure 6, curve *1*), it can be seen that deviation from the linear segment for a single tape is caused by the emerging resistive state and takes place above the critical current I_c, and VAC deviation from the linear inductive segment of the bifilar tape (Figure 6, curve *1*) starts much earlier and is caused by the shift between the tapes and an increase in the inductance of the bifilar segment. Comparison of signals in various sample segments (curves *1*, *2*) shows that, when the current increases, transition to the normal state (a segment with negative slope on curve *1*) starts in the HTSC tape segment to the current lead with the thermal breakdown current of 430 A. Then the normal zone in this segment proliferates, its temperature and resistance grow, which causes reduction of current I, whilst there is no normal zone in the bifilar segment and the signal V_{bif} returns to the initial inductive level. Consequently, the forces that occur between the bifilar tapes are elastic, don't induce heat releases and normal zone nucleation. Therefore, the mechanical position fixation method used for the bifilar tapes turned out to be sufficient for maintaining the superconducting properties of the HTSC material, when the current is applied, up to the point of thermal breakdown current. Inductive reactance of the bifilar segment is 1.33 $\mu\Omega$, however, the reactance level weakly depends on whether the HTSC layers are placed inward or outward in the tapes. As a result of the opposite current flow, the inductive reactance per unit length of the bifilar structure decreased by 14 times compared with a single wire reactance.

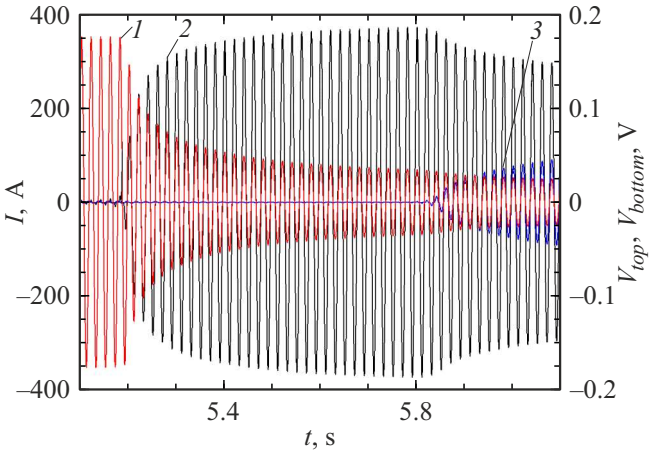

Figure 7. Oscillograms of current and voltage signals from various bifilar segments: *1* — current $I(t)$, *2* — $V_{top}(t)$ signal from the top bifilar tape, *3* — $V_{bottom}(t)$ signal from the bottom bifilar tape.

Table 2. t_R measurement versions in bifilar HTSC tapes

Option No.	5	6	7
HTSC layers in the bifilar wire are brought together(+)/spaced out(−)	+	+	−
External heat insulation of the bifilar wire is present(+)/is absent (-)	−	+	+

The studied bifilar version was used as the basis for creating an extended bifilar line model, one segment of which was raised vertically and placed on a cylinder with a radius of 32 mm [32]. Current was supplied into the system in the same way as for short samples (Figure 1) using transformer power supply. When the nitrogen level decreased, the top of bifilar wire turned out to be in the nitrogen vapor and the normal zone was generated in it. A typical view of such transition starting from the initial current amplitude of 350 A with the nitrogen level lower than the upper bifilar point by 18 mm (with the exposed bifilar length equal to about 70 mm) is shown in Figure 7. The figure shows that heating by means of reduced heat transfer and elevated nitrogen vapor temperature induces the resistive state in the top bifilar tape, then heat releases in the resistive state and heat input from the nitrogen vapor lead to transition of the top bifilar point to the normal state. Then intense resistance, heat release and temperature growth starts in the top tape. After 0.7 s, heating in the tape achieves such value where the heat flux through the insulation between the tapes raises significantly the temperature in the bottom tape, and the normal zone is also generated there. This reduces the voltage and heat release in the top tape, which in turn decelerates or stops the tape temperature growth.

Dependence of the difference of top and bottom tape actuation times t_R on the initial current amplitude I_i for

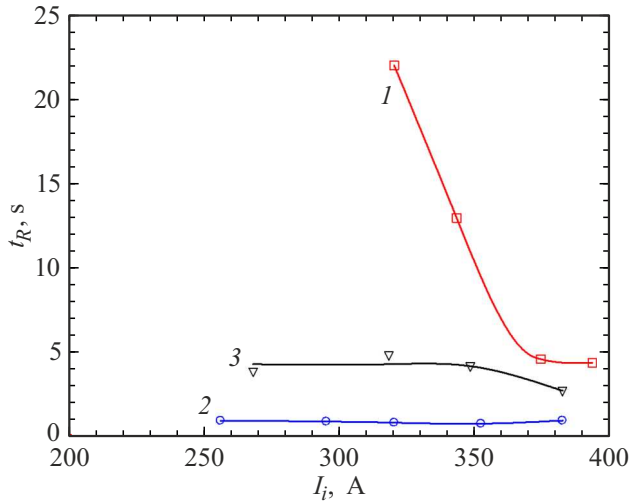

Figure 8. Dependences of the time of the normal zone passage between the bifilar tapes on the initial current amplitude I_i: *1* — option 5; *2* — option 6; *3* — option 7 (measurement options are numerated according to Table 2).

different HTSC tape options (Table 2) in the bifilar wire is shown in Figure 8. Curve *1* (option 5) — bifilar tapes face each other such that their superconducting layers are at a minimum distance of 0.1 mm and are separated only by a fiberglass mesh insulation with nitrogen vapor in mesh cells [49]; moreover, external insulation consisting of adhesive paper tapes is removed near the top bifilar point in the length of 42 mm. Curve *2* (option 6) — superconducting layers of different tapes as in option 1 are brought together, external insulation is provided throughout the bifilar wire. Curve *3* (option 7) — HTSC tapes are placed so that their layers are outside and, besides the insulation between the tapes, there are two 60 μm Hastelloy substrate layers between them; external insulation is applied throughout the bifilar wire as in option 2. It is apparent that, as the maximum temperature of the normal segment in the top bifilar tape increases, the time of normal zone penetration from the top tape into the bottom tape decreases. Therefore, the trend of functional dependence of the maximum temperature T_m on current may be judged by $t_R(I_i)$. In option 5, T_m grows with the current and achieves its plateau as the current approaches its critical value. In options 6 and 7, T_m weakly depends on the current level. Comparative analysis of the provided options may be used to estimate the thermal protection of each of them. Maximum heating level is known to depend on the specific heat releases and on the heat removal pattern from the „hot“ spot [28]. Option 5 is similar to option 1 for the short sample: there is no external insulation and the normal zone in the long sample is concentrated almost only in the top bifilar tape (t_R is high and the normal zone occurs in the bottom tape only when thermal processes in the top tape have already reached the heat balance). But since the exposed length in the long horizontal wire grows faster as the nitrogen level decreases than in the short sample, the

heat release density in the long wire will be lower, therefore maximum heating of the short sample (curve *3*, Figure 5) is estimated as the upper heating limit of option 5. Also note that successful testing in this option was conducted at the initial currents up to the critical current. And this means that the absence of external insulation and mechanical bond between bifilar tapes in the length of several centimeters doesn't have any considerable effect on performance and response to actuation of the total bifilar line.

Compare curves *2* and *3*. Notwithstanding that thermal conductivity of the Hastelloy substrate is by an order of magnitude lower than that of copper [41], it is by three orders of magnitude higher than that of nitrogen gas. However, comparison of curves *2* and *3* indicates that thermal diffusivity perpendicular to the Hastelloy substrate is lower than that of the space between the tapes. This means that the mesh insulation provides the presence of heat exchange gas in a small space between the tapes where the intense convective heat exchange of heated nitrogen vapor takes place.

Experiment technique was arranged such that critical parameters (in particular, critical current and thermal breakdown current) were measured at the start of each series and the measurements were repeated at the end of each series. For experiments that provided the data shown in Figure 8, no differences in superconducting parameters before and after the measurement series with S-N transitions were found. This means that all options with any initial currents in phase transitions are protected against overheating. Option 6 has a higher protection margin because it has an additional protection method that is enabled faster and consists of the normal zone that occurs in the bottom tape with absorption of the larger fraction of released energy.

4.3. Conclusions

It follows from the foregoing that non-stabilized bifilar HTSC wires can provide the necessary sensitivity when creating gas phase sensors for long nitrogen cryostats. Mesh insulation is placed between the HTSC tapes. Gas coolant in mesh cells provides heat overload protection due to high convective heat transfer between the tapes. For mechanical fixation in the bifilar wire, the tapes were placed between adhesive paper tape layers. When currents exceeded 250 A, the tapes shifted against each other, thus slightly increasing the inductive reactance. Meanwhile, the shift is elastic and doesn't induce heat releases that are sufficient for normal zone nucleation. Note also that investigations were carried out with the largest HTSC tape widths in the manufacturer's dimension range. Thus, in addition to verifying the operating principle, implementation of the necessary current leads and power sources at the maximum operating currents was demonstrated. (Due to the sensor's operating principle, the operating current in the sensor is always below the critical value and long current flow time doesn't induce a change in HTSC tape parameters [50].)

Since the normal zone nucleation and heating pattern during transition is defined by the balance of specific heat releases and heat removal, the main transition parameters with decreasing tape width will change a little, and it will be sufficient to use a narrower HTSC tape with the identical structure if the operating current and power supply and current lead requirements shall be reduced. Dependence of inductive reactance on the tape width is logarithmic [51] and the resistive signal in transition is inversely proportional to the width, i.e. the ratio of effective active signal and inductive background signal will increase as the tape width decreases. To create a distributed horizontal sensor in these conditions, it is possible to use a (narrower) stabilized tape that has a larger overheating protection margin. When creating a bifilar wire, HTSC layers in the tapes shall be placed closer to each other because heat transfer through the Hastelloy layers considerably decelerates the passage of the normal zone between the tapes and decreases the overheating protection of the top tape.

Conclusion

Transient processes in current-carrying HTSC wires have been studied during phase transitions in nonuniform heat removal conditions Such nonuniformity occurs when a part of wire initially fully immersed in liquid nitrogen is surrounded by gas. Such experimental setup was used to physically simulate the operating conditions of HTSC sensors of liquid and gas phase interface in nitrogen. This kind of sensor is required for creating liquid level/gas alarm detectors in nitrogen cryostats for superconducting electrical equipment and is necessary to improve operational reliability. Depending on the type of cryostat (a bulk cryostat for HTSC windings of a transformer/current limiter or a long one for an HTSC cable), the sensor shall generate an unacceptably low cryogen level alarm or a local gas inclusion alarm in the cryogenic cable treatment path.

It is shown that AC power supply of HTSC sensors using a transformer supply provides a significant current drop when a small normal zone is formed in the low heat removal region of the HTSC wire. Thus, not only a warning/alarm signal may be generated for a monitoring and control system, but also wire overheating and degradation may be avoided during transition from the superconducting to normal state, and transition reversibility may be provided.

A set of transition characteristics of current-carrying HTSC wires with various layouts (stabilized/non-stabilized, single/bifilar) has been first obtained using different current lead methods (cooled/uncooled current leads) and for conditions corresponding to the wire arrangement in various types of cryostats (bulk/long). Significance of the findings for applications in the field of superconducting power supply equipment development is in that they may be used as the basis for creating superconducting alarm detectors of deviation from normal operating conditions of cryostat systems for such equipment. To improve

the characteristics of superconducting sensors for alarm detectors, the following configurations are recommended:

— for an unacceptable low cryogen level alarm detector in bulk liquid nitrogen cryostats with boiling temperature at atmospheric pressure, it is reasonable to use configuration options with a stabilized/non-stabilized HTSC wire with liquid nitrogen cooling of the top current lead (options 1 and 3, Table 1);

— for an unacceptable low cryogen level alarm detector in bulk liquid nitrogen cryostats with gauge pressure and variable temperature (below the boiling point), it is reasonable to use an option with a non-stabilized HTSC wire without liquid nitrogen cooling of the top current lead (option 4, Table 1);

— for a nitrogen gas alarm detector in an long cryostat for a HTSC cable, the best parameters are demonstrated by option 6 (Table 2) that uses a bifilar connection with a minimum distance between the HTSC layers and an mesh insulation between the tapes with the minimum heat transfer time between the tapes.

Funding

This study was carried out under state assignment using the facilities of the Shared Research Facility of Lebedev Physical Institute of the Russian Academy of Sciences.

Conflict of interest

The authors declare no conflict of interest.

References

[1] E.P. Volkov, L.S. Fleishman, V.S. Vysotsky, A.A. Nosov, V.V. Kostyuk, V.P. Firsov, S.F. Osetrov, A.N. Kiselev. V sb.: *Innovatsionnye tekhnicheskie resheniya v programme NIOKR PAO „FSK EES“*, pod.red. A.E. Murova (AO „NTC FSK EES“, M., 2016), s. 32 (in Russian).

[2] V.V. Zubko, S.Yu. Zanegin, S.S. Fetisov, V.S. Vysotsky, A.A. Nosov, E.S. Otabe, T. Akasaka. Sverkhprovodimost': fundamental'nye i prikladnye issledovaniya **1**, 1 (53) (in Russian). DOI: 10.62539/2949-5644-2024-0-1-53-62

[3] T. Masuda, M. Watanabe, T. Mimura, M. Tanazawa, H. Yamaguchi. J. Phys.: Conf. Ser., **1559**, 012083 (2020). DOI: 10.1088/1742-6596/1559/1/012083

[4] V.R. Romanovskii. Tech. Phys., **60** (1), 86 (2015). DOI: 10.1134/S106378421501020X

[5] V.A. Malginov, A.V. Malginov, L.S. Fleishman, A.S. Rakitin. Tech. Phys., **62** (10), 1516 (2017). DOI: 10.1134/S1063784217100176

[6] D.A. Grigor'ev, O.Yu. Gusev, Yu.P. Gusev, N.O. Posokhov. Therm. Eng., **70** (8), 624 (2023). DOI: 10.1134/S0040601523080037

[7] V.A. Malginov, A.V. Malginov, L.S. Fleishman. Tech. Phys., **64** (12), 1759 (2019). DOI: 10.1134/S106378421912017X

[8] V.A. Malginov, L.S. Fleishman. Tech. Phys. Lett., **50** (4), 71 (2024). DOI: 10.61011/PJTF.2024.08.57518.19785

[9] V.S. Vysotsky, S.S. Fetisov, A.A. Nosov. *Sposob i ustroistvo dlya ohlazhdeniya kabelya* (Patent RF RU 2491671, 27.08.2013 Byul. № 24) (in Russian)

[10] V.G. Fastovsky, Yu V. Petrovsky, A.E. Rovinsky, *Kriogennaya tekhnika* (Energiya, M., 1974) (in Russian)

[11] V.M. Zakosarenko, O.A. Kleshnina, V.N. Tsikhon. V sb.: *Trudy FIAN. Tom 121. Voprosy prikladnoy sverhprovodimosti*, pod red. N.G. Basova (Nauka, M., 1980), s 109 (in Russian).

[12] K.R. Efferson. Adv. Cryogenic Eng., **15**, 124 (1995). DOI: 10.1007/978-1-4757-0513-3_18

[13] J.X. Jin, H.K. Liu, C. Grantham, S.X. Dou. In: *Advances in Cryogenic Engineering. A Cryogenic Engineering Conference Publication*, ed. by P. Kittel (Springer, Boston, MA, 1996), v. 41. DOI: 10.1007/978-1-4613-0373-2_228

[14] K. Kajikawa, K. Tomachi, N. Maema, M. Matsuo, S. Sato, K. Funaki, H. Kumakura, K. Tanaka, M. Okada, K. Nakamichi. J. Phys.: Conf. Ser., **97**, 012140 (2008). DOI: 10.1088/1742-6596/97/1/012140

[15] K. Tomachi, K. Kajikawa, M. Matsuo, S. Sato, K. Tanaka, K. Funaki, H. Kumakura, M. Okada, K. Nakamichi, Yu. Kihara, T. Kamiya, I. Aoki. J. Cryogenics and Superconductivity Society Jpn., **44** (8), 366 (2009). DOI: 10.2221/jcsj.44.366

[16] K. Matsumoto, M. Sobue, K. Asamoto, Y. Nishimura, S. Abe, T. Numazawa. Cryogenics, **51** (2), 114 (2011). DOI: 10.1016/j.cryogenics.2010.11.005

[17] K. Kajikawa, T. Inoue, K. Watanabe, M. Kanazawa, Yu. Yamada, H. Kobayashi, H. Taguchi, I. Aoki. Phys. Proced., **36**, 1396 (2012). DOI: 10.1016/j.phpro.2012.06.311

[18] M.A. Kolosov, V.Yu. Yemelyanov, E.S. Navasardyan. Vestnik MGTU im. N.E. Baumana. Ser. Mashinostroenie, **6**, 116 (2014) (in Russian).

[19] K. Kajikawa, T. Inoue. K. Watanabe. Yu. Yamada, I. Aoki. AIP Conf. Proc., **1573**, 905 (2014). DOI: 10.1063/1.4860800

[20] R. Karunanithi, S. Jacob, D.S. Nadig, M.V.N. Prasad, A.S. Gour, M. Gowthaman, P. Deekshith, V. Shrivastava. AIP Conf. Proc., **1573**, 913 (2014). DOI: 10.1063/1.4860801

[21] R. Karunanithi, S. Jacob, D.S. Nadig, M.V.N. Prasad, A.S. Gour, S. Pankaj, M. Gowthaman, H. Sudharshan. Phys. Proced., **67**, 1169 (2015). DOI: 10.1016/j.phpro.2015.06.182

[22] K. Maekawa, M. Takeda, Yu. Matsuno, S. Fujikawa, T. Kuroda, H. Kumakura. Phys. Proced., **67**, 1164 (2015). DOI: 10.1016/j.phpro.2015.06.181

[23] K. Maekawa, M. Takeda, T. Hamaura, K. Suzuki, Yu. Matsuno, S. Fujikawa, H. Kumakura. IEEE Trans. Appl. Supercond., **27** (4), 9000304 (2017). DOI: 10.1109/TASC.2016.2642048

[24] A.S. Gour, P. Sagar, R. Karunanithi. Cryogenics, **84**, 76 (2017). DOI: 10.1016/j.cryogenics.2017.04.007

[25] K.R. Kunniyoor, T. Richter, P. Ghosh. R. Lietzow, S. Schlachter, H. Neumann. IEEE Trans. Appl. Supercond., **28** (2), 9000810 (2018). DOI: 10.1109/TASC.2018.2799144

[26] J.M. Mun, J.H. Lee, S.C. Lee, R.D. Sim, S.H. Kim. Progress in Superconductivity and Cryogenics, **23** (4), 56 (2021). DOI: 10.9714/psac.2021.23.4.056

[27] X. Chi, X. Wang, X. Ke. Micromachines, **13** (4), 633 (2022). DOI: 10.3390/mi13040633

[28] A.V. Gurevich, R.G. Mints, A.L. Rakhmanov. *The Physics of Composite Superconductors* (Begell house inc., NY., 1997)

[29] V.A. Malginov, L.S. Fleishman, D.A. Gorbunova. Supercond. Sci. Technol., **33** (4), 045008 (2020). DOI: 10.1088/1361-6668/ab7470
[30] M.N. Wilson. *Superconducting magnets* (Clarendon Press, Oxford, 1983)
[31] A. Ivanov-Smolensky. *Electrical Machines* (Mir Publishers, Moscow, 1982), v. 1.
[32] V.A. Malginov, L.S. Fleishman. Tech. Phys. Lett., **51** (4), 81 (2025). DOI: 10.61011/TPL.2025.04.61008.20141
[33] A. Goyal (editor). *Second-Generation HTS Conductors* (Kluwer Academic Publishers, Norwell, 2005)
[34] S. Samoilenkov, A. Molodyk, S. Lee, V. Petrykin, V. Kalitka, I. Martynova, A. Makarevich, A. Markelov, M. Moyzykh, A. Blednov. Supercond. Sci. Technol., **29** (2), 024001 (2016). DOI: 10.1088/0953-2048/29/2/024001
[35] W.J. Carr Jr. *AC Loss and Macroscopic Theory of Superconductors* (Taylor & Francis, L., 2001)
[36] W. Frost. *Heat Transfer at Low Temperatures* (Springer Science, NY., 1975)
[37] V.A. Grigoriev, Yu.M. Pavlov, E.V. Ametistov. *Kipenie kriogennykh zhidkostei* (Energiya, M., 1977) (in Russian)
[38] S.S. Fetisov, V.S. Vysotsky, V.V. Zubco. IEEE Trans. Appl. Supercond., *21* (3), 1323 (2011). DOI: 10.1109/TASC.2010.2093094
[39] V.A. Malginov, A.V. Malginov, L.S. Fleishman. Tech. Phys. Lett., **45** (4), 331 (2019). DOI: 10.1134/S1063785019040096
[40] E.P. Volkov, E.A. Dzhafarov, L.S. Fleishman, V.S. Vysotsky, V.V. Sukonkin. Therm. Eng., **63** (13), 909 (2016). DOI: 10.1134/S0040601516130085
[41] S.V. Pokrovsky, A.Yu. Malyavina, R.G. Batulin, I.A. Rudnev. Kabeli i provoda **6**, 14 (2023) (in Russian). DOI: 10.52350/2072215X_2023_6_14
[42] M.P. Malkov (red.). *Spravochnik po fiziko-tekhnicheskim osnovam kriogeniki* (Energoatomizdat, M., 1985) (in Russian)
[43] A.V. Malginov, A.Yu. Kuntsevich, V.A. Malginov, L.S. Fleishman. J. Exp. Theor. Phys., **117** (6), 1078 (2013). DOI: 10.1134/S106377611314015X
[44] *Bulk Liquid Oxygen, Nitrogen, and Argon Storage Systems at Production Sites* (European Industrial Gases Association AISBL, Brussels, Doc 127/23)
[45] Y. Yue, G. Chen, J. Long, L. Ren, K. Zhou, X. Li, Y. Xu, Y. Tang. Superconductivity, **4**, 100028 (2022). DOI: 10.1016/j.supcon.2022.100028
[46] Yu. Larin, Yu. Smirnova. Pervaya milya, **1**, 16 (2011). (in Russian)
[47] X. Li, C. Qian, R. Shen, H. Xiao, S. Ye. Opt. Express, **28** (6), 8233 (2020). DOI: 10.1364/OE.384994
[48] S.S. Fetisov, D.V. Sotnikov, S.Yu. Zanegin, N.V. Bykovsky, I.P. Radchenko, V.V. Zubko, V.S. Vysotsky. Phys. Proced., **67**, 931 (2015). DOI: 10.1016/j.phpro.2015.06.157
[49] V.A. Malginov, L.S. Fleishman. Tech. Phys. Lett., **49** (6), 50 (2023). DOI: 10.61011/TPL.2023.06.56380.19579
[50] S. Veselova, M. Osipov, A. Starikovskii, I. Anishenko, S. Pokrovskii, D. Abin, I. Rudnev. J. Phys.: Conf. Ser., **1975**, 012015 (2021). DOI: 10.1088/1742-6596/1975/1/012015
[51] P.L. Kalantarov, L.A. Tseytlin. *Raschet induktivnostey: spravochnaya kniga* (Energoatomizdat, L., 1986) (in Russian)

Translated by E.Ilinskaya